

*Plutonium Scrap Multiplicity Counter  
Operation Manual*

*H. O. Menlove*

*J. Baca*

*M. S. Krick*

*K. E. Kroncke*

*D. G. Langner*

**Los Alamos**  
NATIONAL LABORATORY

Los Alamos, New Mexico 87545

**MASTER**

RP

THIS DOCUMENT IS UNCLASSIFIED

## CONTENTS

ABSTRACT .....	1
INTRODUCTION .....	2
GENERAL.....	2
DESIGN FEATURES .....	2
DETECTOR DESCRIPTION .....	5
PERFORMANCE CHARACTERISTICS .....	9
GENERAL.....	9
HIGH-VOLTAGE PLATEAU .....	9
DIE-AWAY TIME .....	10
DETECTOR DEADTIME.....	10
MULTIPLICITY DEADTIME .....	11
EFFICIENCY .....	11
MATRIX EFFECTS .....	12
CONTAINER EFFECTS.....	13
AXIAL PROFILES .....	14
RADIAL PROFILES .....	14
PRECALIBRATION FOR SMALL SAMPLES.....	16
PRECALIBRATION .....	16
SUMMARY .....	19
ACKNOWLEDGMENTS .....	21
REFERENCES .....	21

# **PLUTONIUM SCRAP MULTIPLICITY COUNTER OPERATION MANUAL**

by

H. O. Menlove, J. Baca, M. S. Krick, K. E. Kroncke, and D. G. Langner

## **ABSTRACT**

This manual describes the design features and performance and operating characteristics for the plutonium scrap multiplicity counter (PSMC). It counts neutron multiplicities to quantitatively assay plutonium in many forms, including impure scrap and waste. Monte Carlo neutronic calculations were used to design the high-efficiency (55%) detector using eighty  $^3\text{He}$  tubes in a high-density polyethylene body. The new multiplicity shift-register electronics can sort multiplicities up to 256. The PSMC can be applied to plutonium masses in the range from a few milligrams to 5 kg; both conventional coincidence counting and multiplicity counting are used as appropriate. This manual gives the performance data and preliminary calibration parameters for the PSMC.

---

**GENERAL**

The plutonium scrap multiplicity counter (PSMC) is a high-efficiency neutron counter designed for measuring the multiplicity of the neutron emission from both spontaneous fission and induced-fission reactions in plutonium and uranium. The PSMC can also be used to measure the neutron multiplicity from the spontaneous fission in curium.

The PSMC was developed to measure impure plutonium and mixed-oxide (MOX) scrap materials that are under International Atomic Energy Agency (IAEA) inspection. We performed basic research for and design of the PSMC hardware and software under the Department of Energy safeguards research program. The Program of Technical Assistance to IAEA Safeguards funded PSMC fabrication and implementation.

The PSMC will be applied to impure plutonium and MOX samples that range in mass from a few tens of grams to several kilograms of high-burnup plutonium. The PSMC also can be used for the assay of subgram inventory samples that have been bagged out of glove boxes.

**DESIGN FEATURES**

The PSMC evolved from multiplicity neutron detectors<sup>1,2</sup> developed at Los Alamos for impure plutonium samples. The new unit was designed to be more compact and to use fewer <sup>3</sup>He tubes to obtain a high efficiency. We designed the PSMC by using the Monte Carlo Code for Neutron and Photon Transport (MCNP) to perform the Monte Carlo neutron calculations.<sup>3</sup> The design goals for the PSMC were

1. high efficiency (primary importance),
2. uniform efficiency vs. sample height,
3. small die-away time,
4. flat energy response,
5. minimum number of <sup>3</sup>He tubes, and
6. minimum overall size and weight.

The first four of these design goals work in opposition to the last two. However, the MCNP calculations provided data to significantly improve on the prior designs. For example, the pyrochemical detector<sup>2</sup> used one hundred twenty-six <sup>3</sup>He tubes to obtain an efficiency of 57%, whereas the present

**DESIGN FEATURES**

(cont.)

design uses eighty  $^3\text{He}$  tubes to get an efficiency of 55%, but with slight degradations in the die-away time and the energy response.

Figure 1 shows a schematic diagram of the PSMC design with the eighty  $^3\text{He}$  tubes surrounding the sample cavity with a diameter of 20 cm. The outer dimensions of the polyethylene ( $\text{CH}_2$ ) shield are 66 by 66 by 80 cm. The total height is 92 cm. The number of  $^3\text{He}$  tubes was reduced in direct proportion to the decrease in the thermal-neutron flux density in the  $\text{CH}_2$  moderator. Thus, the tube density is much higher

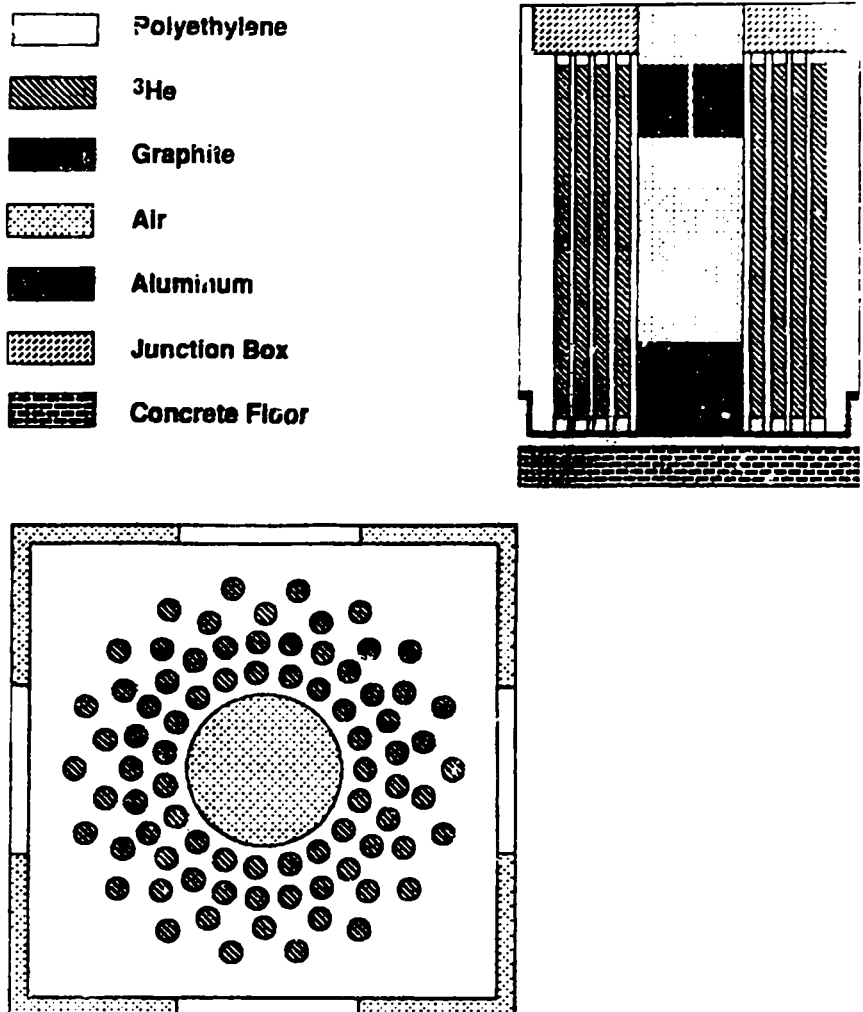


*Fig. 1. Schematic diagram of the PSMC showing the location of the eighty  $^3\text{He}$  tubes and the graphite end plugs. The sample cavity height is 41 cm and the diameter is 20 cm.*

DESIGN FEATURES  
(cont.)

in the first ring of tubes near the sample cavity than in the fourth ring of tubes away from the sample.

The sample cavity is lined with cadmium (0.8 mm thick) both to prevent thermalized neutrons from returning from the CH<sub>2</sub> into the sample and inducing fission reactions and to shield the <sup>3</sup>He tubes from a possible high-intensity gamma-ray dose from high-burnup plutonium samples. There is no cadmium on the outside of the detector rings to reduce room-background levels. MCNP calculations<sup>4</sup> have shown that cadmium only reduces the totals background rate by ~16%, and the cadmium introduces its own background of coincident neutrons from cosmic-ray spallations. The end plugs shown in Fig. 1 are made of graphite to scatter the fast neutrons from the end zones back into the CH<sub>2</sub> detector volume.

The MCNP calculation of the response of the detector system as a function of neutron energy is shown in Fig. 2, along with the comparison curve from the pyrochemical counter.<sup>2</sup> The majority of spontaneous fission and ( $\alpha$ ,n) reaction neutrons have energies in the range of 0.5–2 MeV.

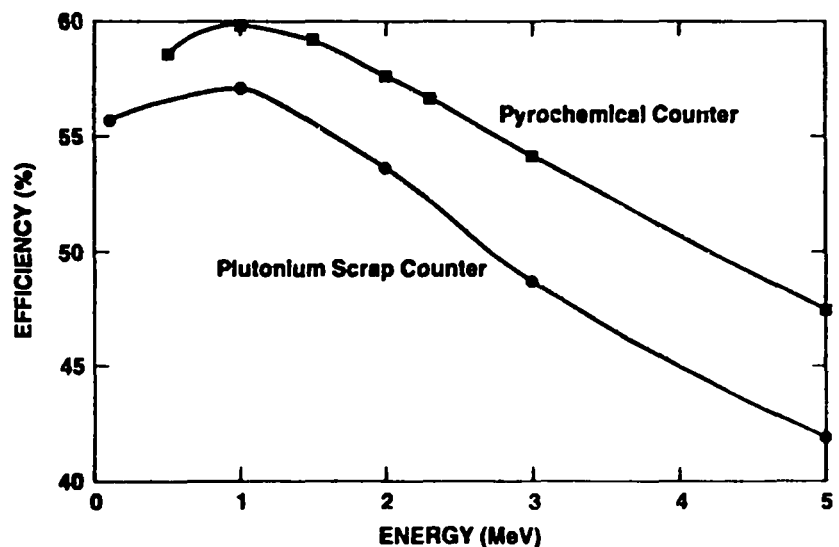
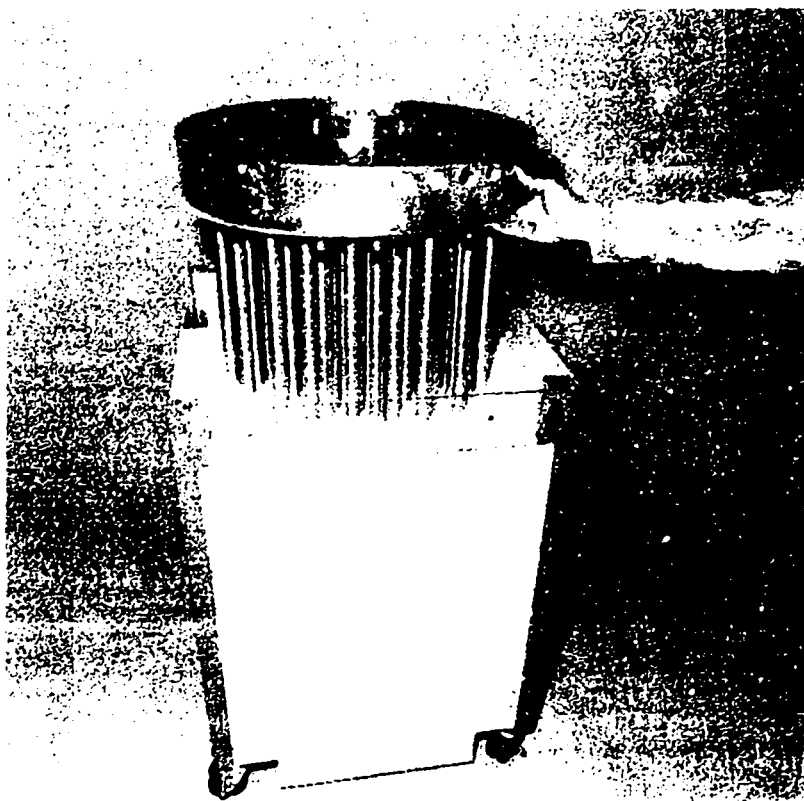


Fig. 2. MCNP calculations of the efficiency vs the neutron energy for the PSMC and the pyrochemical counter.<sup>2</sup>

## DETECTOR DESCRIPTION

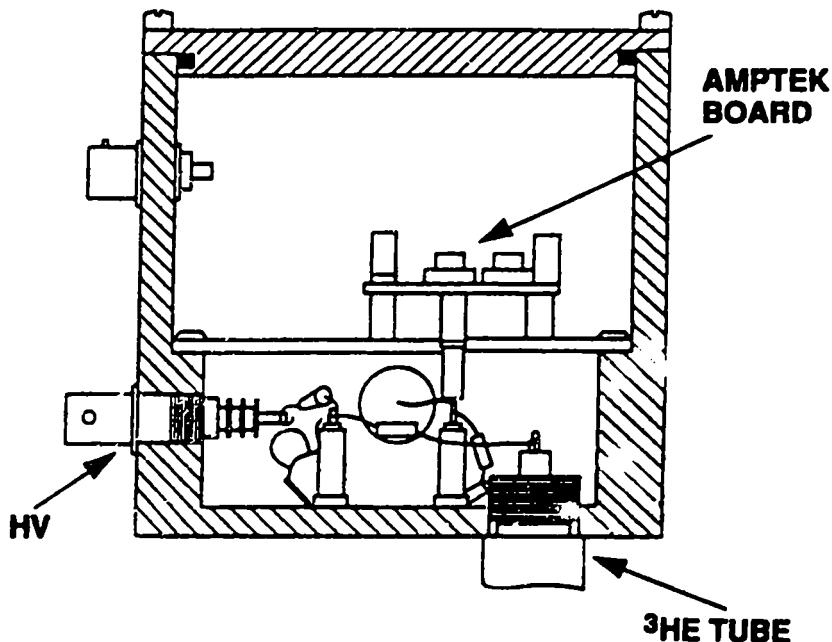
The eighty  $^3\text{He}$  tubes have an active length of 71 cm with the specifications given in Table I. The  $^3\text{He}$  tubes partially withdrawn from the  $\text{CH}_2$  are shown in Fig. 3. The  $^3\text{He}$  tubes are connected to the AMPTEK amplifiers<sup>5</sup> as shown in Fig. 4. To give approximately equal counting rates to each

Table I. Helium-3 Tube Parameters	
Model	RS-P4-0828-101
Active length	71 cm
Diameter	2.54 cm
Fill pressure	4 atm
Gas quench	Argon + $\text{CH}_4$
Cladding	Aluminum
Operating voltage	1680 V



*Fig. 3. Photograph of the  $^3\text{He}$  tubes and high-voltage junction box partly withdrawn from the PSMC.*

**DETECTOR DESCRIPTION**  
(cont.)



*Fig. 4. Schematic diagram of the relationship between the  $^3\text{He}$  tubes and the AMPTEK amplifier board in the high-voltage junction box. The PSMC contains 19 AMPTEK boards inside a larger high-voltage box than depicted in Fig. 4.*

AMPTEK amplifier, fewer tubes are connected to each amplifier for the inside tube ring than for the outer rings. For example, one amplifier services three tubes on the innermost ring and six tubes on the outside rings. Figure 5 shows the measured counting rate from each AMPTEK amplifier for a  $^{252}\text{Cf}$  source in the center of the sample cavity. This demonstrates the decrease in the neutron flux density with distance into the  $\text{CH}_2$ .

The 19 AMPTEK amplifiers that are used with the PSMC are shown in Fig. 6. The amplifier boards are electrically isolated from the detector signal lines by an aluminum grounding plate also shown in Fig. 6. Each of the 19 amplifiers has a digital output signal that causes a light-emitting diode, shown in Fig. 7, to blink. The twentieth signal light indicates the status of the 5-V power supply for the amplifier boards.



# DETECTOR DESCRIPTION

(cont.)

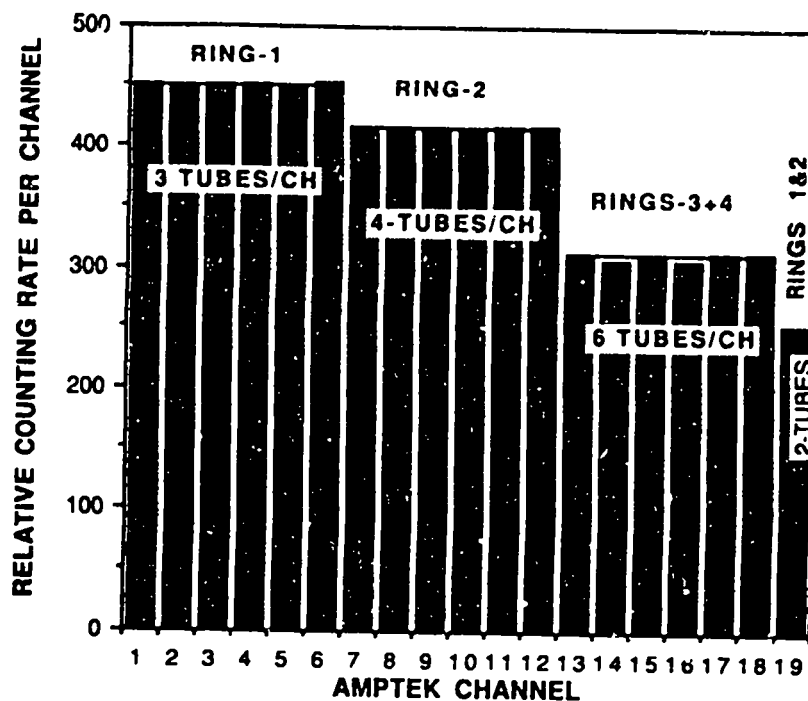


Fig. 5. Measured counting rates from the 19 individual AMPTEK boards for a central neutron source in the PSMC showing the number of tubes connected to each amplifier.

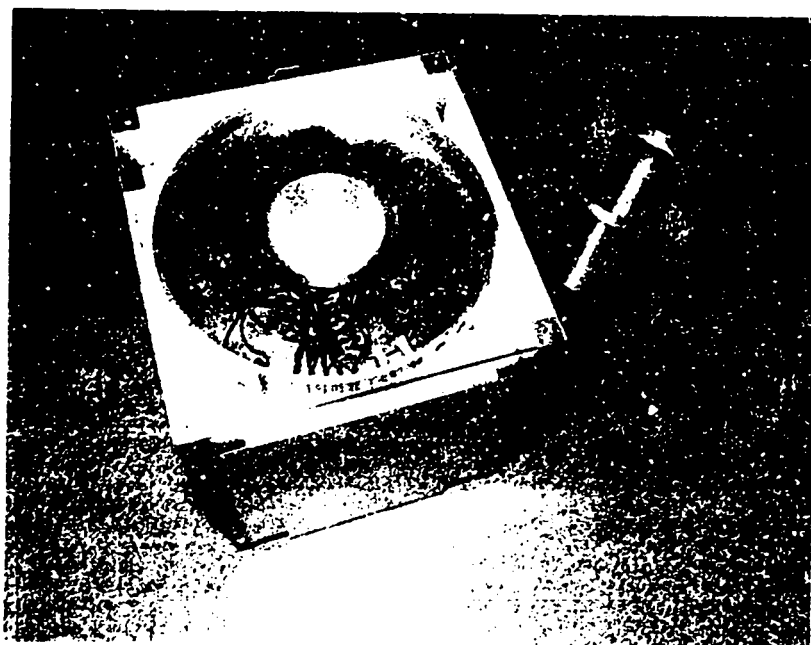
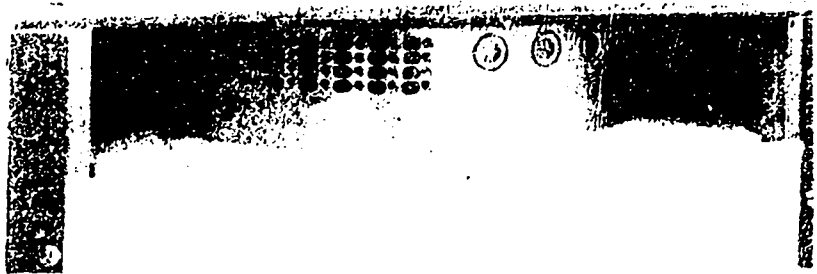


Fig. 6. Photograph of the high-voltage junction box including the AMPTEK boards.

**DETECTOR DESCRIPTION**

(cont.)



*Fig. 7. Side view of the LED lights that connect to the AMPTEK board and the four desiccant tubes in the PSMC.*

Figure 7 also shows the four removable desiccant tubes that are used to keep the detector high-voltage box dry.

The assembled PSMC detector is shown in Fig. 8.

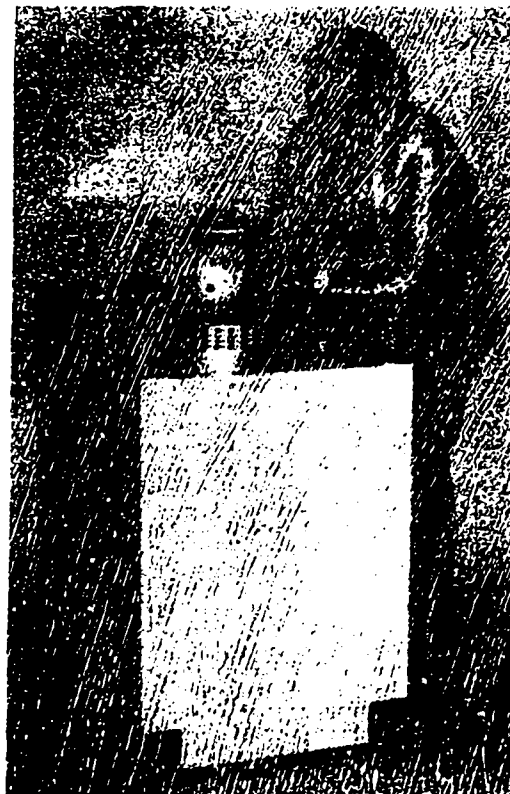


*Fig. 8. Photograph of the assembled PSMC.*

**GENERAL**

A series of measurements was taken to evaluate the performance of the detector. They consisted of measuring the high-voltage plateau, the neutron die-away time, the deadtime, and the absolute efficiency of the detector.

**HIGH-VOLTAGE PLATEAU**

The high-voltage plateau was measured using a californium source. The high voltage was started at 1500 V and incremented by 20 V for each successive measurement until 1900 V was reached. At each voltage, the totals rate was measured. The data are shown in Fig. 9. The knee occurred at 1640 V. The operating voltage is shown to be 1680 V, 40 V above the knee.

An  $^{241}\text{Am}$  sample with a high-dose rate of 500 mR/h at the surface was measured as a function of high-voltage setting to evaluate gamma-ray interference problems. As can be seen in Fig. 9, there is no interference problem for 500 mR/h at an operating voltage of 1680 V.

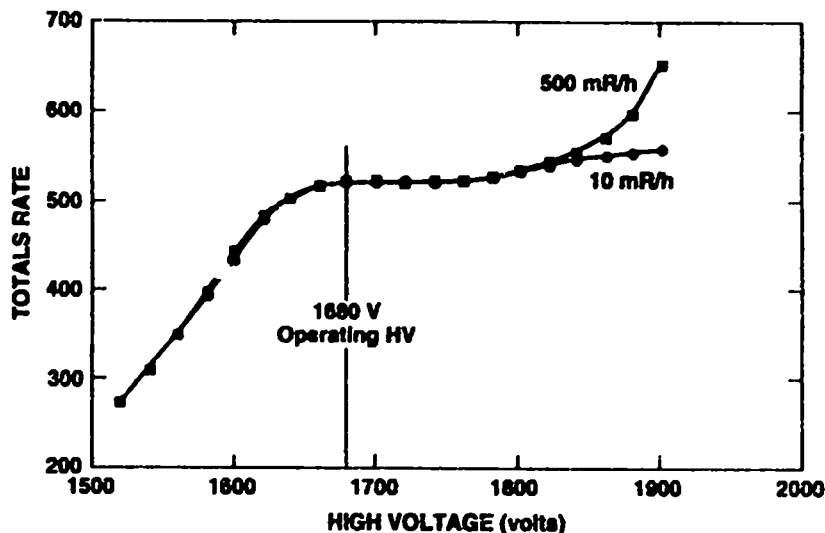


*Fig. 9. High-voltage plateau for the PSMC including a second plateau measured under high gamma-ray background conditions (500 mR/h).*

**DIE-AWAY TIME**

We used a  $^{252}\text{Cf}$  source and gate settings ranging from 8 to 128  $\mu\text{s}$  to measure the average die-away time of the PSMC to be

$$\tau = 47 \mu\text{s} .$$

**DETECTOR DEADTIME**

The PSMC can be used in both the conventional (two-parameter) coincidence counting mode and in the multiplicity mode. The deadtime considerations are much more complex for the multiplicity mode.

For the simple coincidence mode, the deadtime coefficient  $\delta$  is given by

$$\delta = (a + bT \cdot 10^{-6}) \mu\text{s} ,$$

where  $T$  is the measured totals rate in counts/s and  $a$  and  $b$  are constants given in Table II. The corrected counting rates are

$$T(\text{corr.}) = T e^{\delta T/4}$$

and

$$R(\text{corr.}) = R e^{\delta T} .$$

It is important to use the same deadtime coefficient for both calibration and assay so that any errors in the correction will cancel to a first approximation.

**DETECTOR DEADTIME**  
(cont.)

TABLE II. PSMC Performance Characteristics (Date: May 21, 1991)	
Parameter	WDAS
Efficiency	55.0%
Die-away time (center)	47 $\mu$ s
Gate setting	32 $\mu$ s
High voltage	1680 V
Deadtime coefficient <i>a</i>	0.409 $\mu$ s
Deadtime coefficient <i>b</i>	0.122 $\mu$ s
<i>T</i> (CR-5) on May 21, 1992	4754 counts/s
<i>R</i> (CR-5) on May 21, 1992	2556 counts/s

**MULTIPLICITY DEADTIME**

For multiplicity analysis, the deadtime corrections are done with the equations derived by Dytlewski<sup>7</sup> using a constant deadtime *d*. The value of *d* was determined by measuring several <sup>252</sup>Cf sources with different neutron source strengths. The triples/doubles multiplicity ratio should be independent of the neutron source strength after deadtime correction. The value of *d* that gave the best average was

$$d = 121 \text{ ns} .$$

**EFFICIENCY**

The efficiency for the PSMC was measured using a calibrated <sup>252</sup>Cf source (CR-5) on May 21, 1992, and the result was

$$\epsilon = \frac{4754 \text{ s}^{-1}}{8638 \text{ n/s}} = 0.550 .$$

The efficiency measurement was repeated after field installation and the result was

$$\epsilon = 0.541 .$$

## MATRIX EFFECTS

To determine the effects of different matrices on the measurement, a californium source was placed in a 10-cm-diam can filled by a matrix. The can setup is shown in Fig. 10, and the data are displayed in Fig. 11. The graph shows that the detector is fairly immune to the neutron energy moderation in most matrix materials.

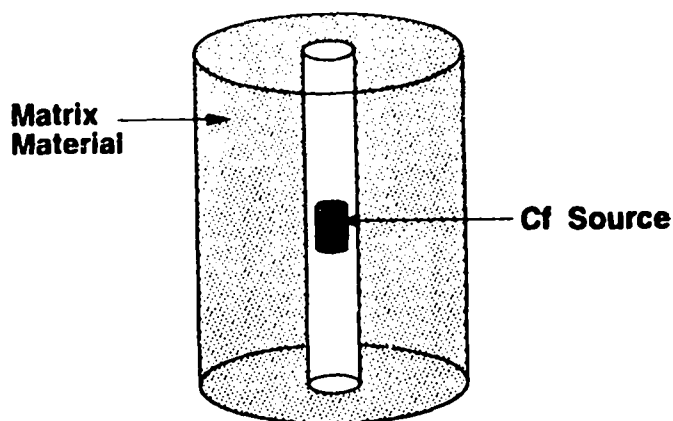


Fig. 10. Neutron source and can geometry for measuring the matrix effects on the counting efficiency.

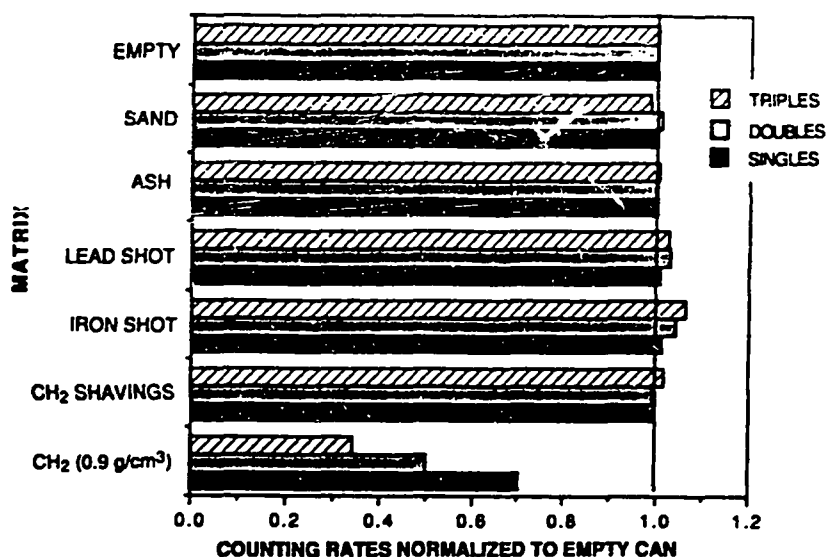


Fig. 11. Results of the matrix study for singles, doubles, and triples normalized to the empty can case.

## CONTAINER EFFECTS

The effects of the container walls were evaluated by placing a californium source in a steel can with various wall thicknesses. The experimental setup is shown in Fig. 12, and the data are shown in Fig. 13. The graph can be used to correct

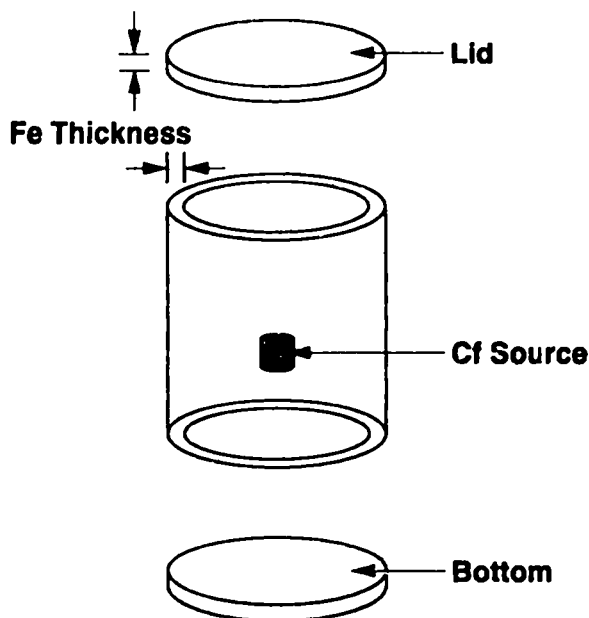


Fig. 12. Can geometry for measuring the effect of iron can walls on the response.

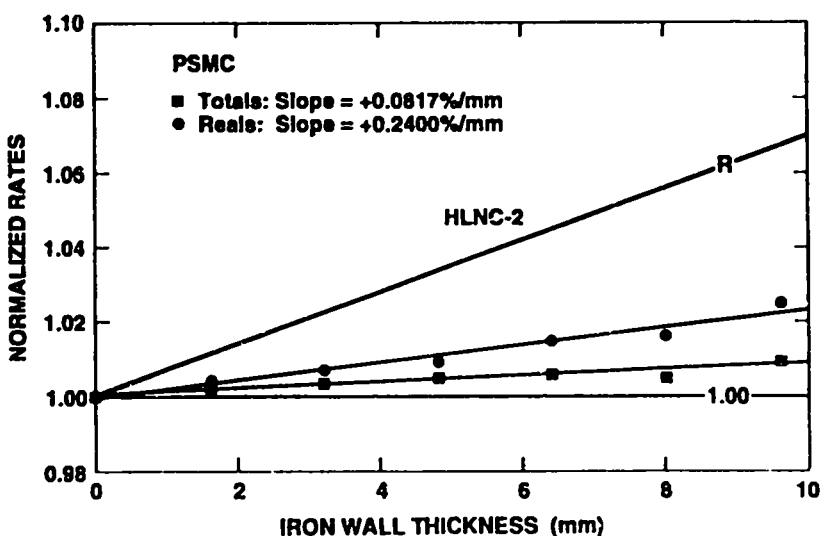


Fig. 13. Results of the test for the effect of the iron-can-wall thickness on the singles and doubles rates normalized to unity for zero wall thickness. The HLNC-II results are included for comparison.

**CONTAINER EFFECTS**  
(cont.)

measurement data for wall effects. The efficiency correction is very small,  $\leq 0.5\%$  for normal sample cans. The data for an HLNC-II are shown in Fig. 12 for comparison with the PSMC. In general, the container material and thickness have a negligible effect on the PSMC results.

A  $^{252}\text{Cf}$  point source of neutrons was used to measure the axial and radial response profiles for the PSMC.

**AXIAL PROFILES**

The axial efficiency profile (see Fig. 14) varies by less than  $\pm 2\%$  over the height (41 cm) of the cavity and the coincidence (doubles) profile falls within the  $\pm 2\%$  boundaries over practical sample fill heights. Of course, the integral response for a can of plutonium has less variation than the measured  $^{252}\text{Cf}$  point source.

**RADIAL PROFILES**

The same  $^{252}\text{Cf}$  source was used to measure the radial response variation at the midplane of the sample cavity. The results are shown in Fig. 15 for the totals and reals rates. The efficiency variation is 1.5% over the 16-cm can diameter. In general, the sample can should be centered in the cavity and the integral radial variations will be  $< 1\%$ .

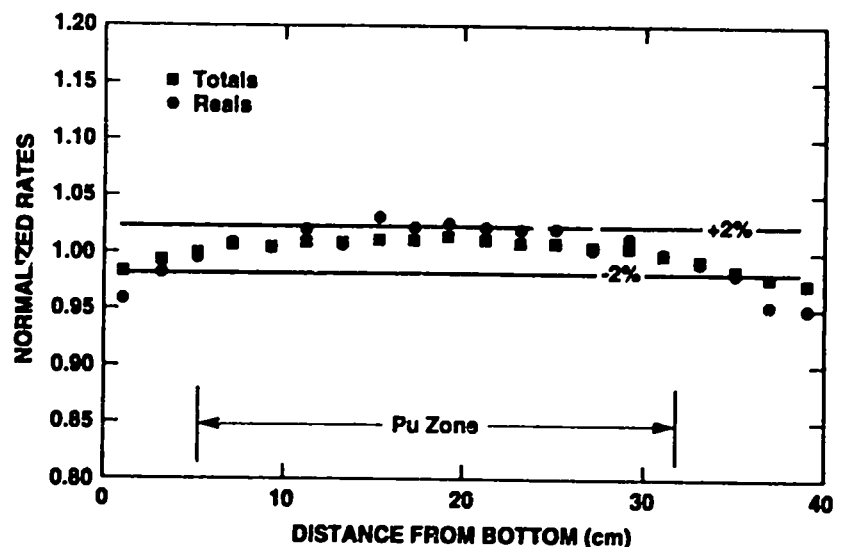


*Fig. 14. Measured reals and totals rates as a function of distance above the bottom of the sample cavity.*



RADIAL PROFILES  
(cont.)

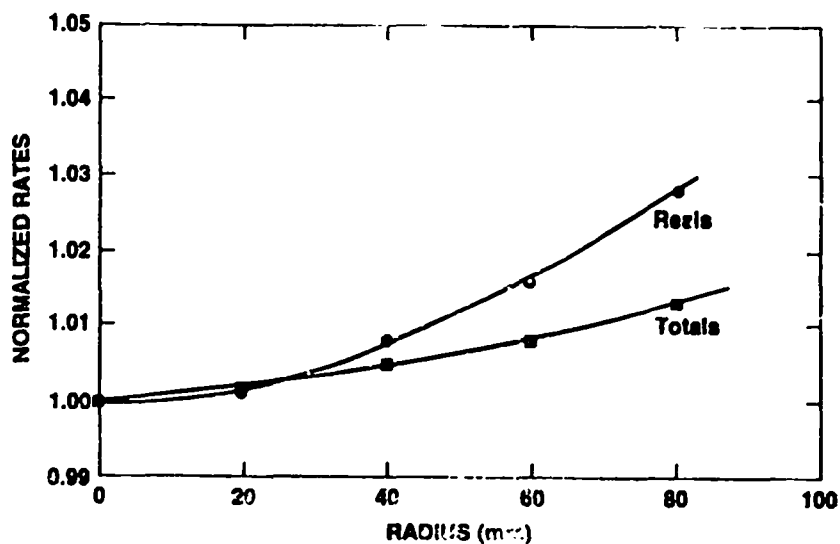


Fig. 15. Measured reals and totals rates as a function of radius from the center of the sample can.

For the conventional two-parameter analysis of neutron coincidence data, it is useful to define the multiplication constant  $\rho_0$  where

$$\rho_0 = \frac{R}{T}(1 + \alpha), \quad (\text{for a nonmultiplying sample}),$$

where  $\alpha$  is the calculated ratio of alpha-particle-induced neutrons to spontaneous fission neutrons.

Small MOX pellets were used to measure  $\rho_0$ , giving

$$\rho_0 = \frac{9.97}{99.39}(1 + 0.01) = 0.200$$

for a predelay of 4.5  $\mu\text{s}$  and a gate length of 32  $\mu\text{s}$ .

The multiplicity analysis does not use the  $\rho_0$  constant.

**PRECALIBRATION  
FOR SMALL SAMPLES**

A preliminary conventional calibration was performed using small MOX pellet standards. The response is described by a straight line through the origin

$$R = a M_{240} ,$$

where  $a = 114.8$  and  $M_{240}$  is the  $^{240}\text{Pu}$ -eff. mass in grams.

$$M_{240} = 2.52 \text{ }^{238}\text{Pu} + \text{}^{240}\text{Pu} + 1.68 \text{ }^{242}\text{Pu} .$$

In this case, the multiplication is negligible and  $\alpha$  is well known.

**PRECALIBRATION**

The  $\text{PuO}_2$  and MOX standards in the mass range of interest are used to calibrate the PSMC. At Los Alamos, we used the standard LAO and PEO sets of  $\text{PuO}_2$  standards for a preliminary calibration.

Table III gives the specifications for the LAO and PEO standards. These samples were measured in the PSMC, and the results are presented in Table IV.

TABLE III. $\text{PuO}_2$ Can Data (as of 3/6/88)											
ID	Reference Date	% 238	% 239	% 240	% 241	% 242	% $^{241}\text{Am}$	Grams Pu	$^{239} + ^{241}\text{Pu}$	g $^{240}\text{Pu}$	$\alpha$
PEO-382B	5/80	0.024	89.70	9.69	0.48	0.11	0.407	74.81	67.47	7.42	0.610
PEO-382C	5/80	0.024	89.70	9.69	0.48	0.11	0.407	149.6	134.9	14.84	0.610
PEO-385	5/80	0.021	90.20	9.27	0.41	0.09	0.346	458.0	415.0	43.35	0.614
PEO-381	5/80	0.029	88.93	10.34	0.58	0.12	0.481	613.2	548.9	65.02	0.601
PEO-447	5/80	0.035	89.09	10.14	0.58	0.16	0.461	776.7	696.4	81.40	0.608
LAO251C10	9/27/83	0.063	82.14	16.39	1.07	0.34	0.368	171.5	142.7	29.31	0.415
LAO252C10	10/3/83	0.055	82.30	16.25	1.04	0.34	0.357	321.1	267.7	54.38	0.411
LAO256C10	10/26/83	0.058	82.28	16.29	1.04	0.34	0.338	314.0	319.9	65.14	0.409
LAO255C10	10/24/83	0.068	82.25	16.29	1.05	0.34	0.351	542.6	451.9	92.22	0.418
LAO261C10	9/22/83	0.058	82.16	16.38	1.07	0.34	0.336	846.7	704.6	144.4	0.407
LAO261C11	9/22/83	0.058	82.16	16.38	1.07	0.34	0.336	874.6	727.9	149.2	0.407

PRECALIBRATION  
(CONT.)

TABLE IV. Neutron Multiplicity Data and Assay Results						
Sample	Moments			<sup>240</sup> Pu-eff (g)	Assay/Reference	
	Singles (s <sup>-1</sup> )	Doubles (s <sup>-1</sup> )	Triples (s <sup>-1</sup> )		Conventional	Multiplicity
PEO382B	7 415.0	891.6	225.4	7.414	1.077	1.018
PEO382D	30 399.1	4 035.8	1 248.0	29.66	1.083	1.013
PEO385	43 452.0	6 273.5	2 135.2	43.33	1.039	1.014
PEO381	65 515.3	9 633.0	3 508.6	64.95	1.052	0.986
PEO447	81 090.2	12 808.2	5 020.0	81.31	1.019	0.997
LAO251C10	24 526.4	3 823.4	1 163.8	29.29	1.009	1.002
LAO252C10	45 743.7	7 668.0	2 635.4	54.33	1.001	1.005
LAO256C10	54 532.7	9 477.8	3 363.5	65.1	0.990	1.018
LAO255C10	78 505.5	14 067.7	5 401.5	92.14	0.991	1.010
LAO261C10	125 044.5	23 781.4	10 625.5	144.3	1.004	0.971
LAO261C11	129 329.3	24 559.9	10 737.8	149.1	1.005	0.989
Average					1.025	1.002
Standard Deviation					0.033	0.015
Percent					3.3	1.5

\*The data were taken with a 3.0-μs predelay and a 64-μs gate.

Table IV presents the counting data for the multiplicity analysis and the assay/reference ratios for both the conventional (two parameter) and multiplicity (three parameter) analyses (64-μs gate). We see that the standard deviation is reduced from 3.3% to 1.5% by using the multiplicity analysis. These results are illustrated in Figs. 16 and 17.

The data given in Table IV and Figs. 16-17 correspond to a 3-μs predelay and a 64-μs gate. To be more conservative in the electronics for high-count-rate applications, we changed from the above parameters to a 4.5-μs predelay and a 32-μs gate for the final calibration.

The small MOX pellets were measured as a group of five pellets and sample A1-078 was measured individually. The results are listed in Table V.

The ash sample (STDASH-1) and the diatomaceous earth sample (STDSGA-100) have α values that are significantly higher than the values calculated for a pure oxide. The

PRECALIBRATION  
(cont.)

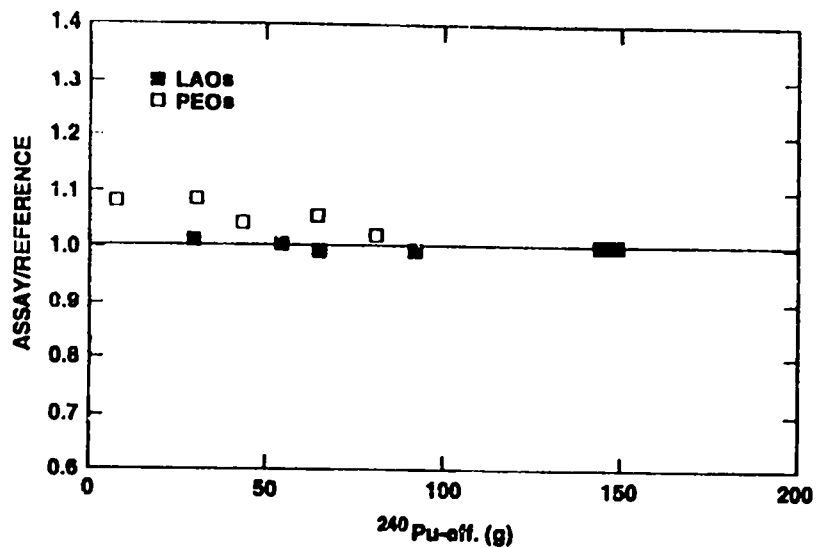


Fig. 16. The assay/reference error vs  $^{240}\text{Pu-eff. mass}$  for pure (LAO) and impure (PEO)  $\text{PuO}_2$  samples using the conventional two-parameter assay.

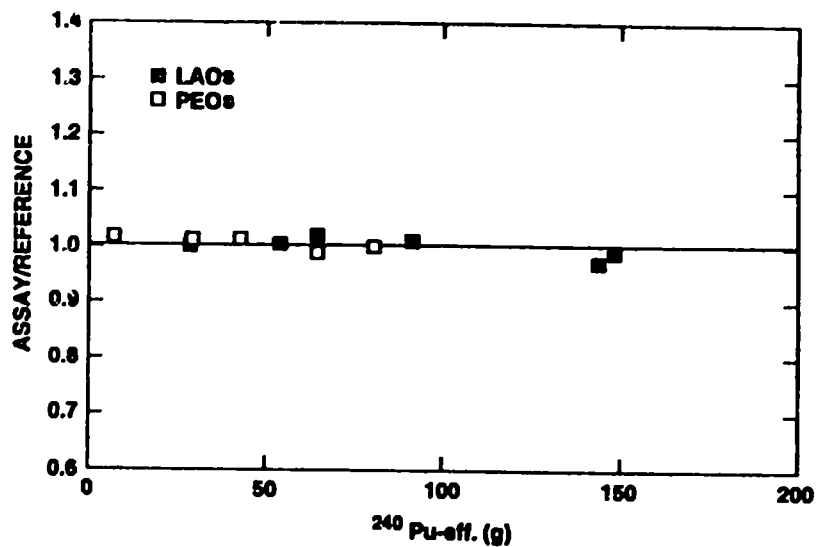


Fig. 17. The assay/reference error vs  $^{240}\text{Pu-eff. mass}$  for pure (LAO) and impure (PEO)  $\text{PuO}_2$  samples using the multiplicity assay.

**PRECALIBRATION**  
(cont.)

TABLE V. Preliminary PSMC Test Data									
Sample	$\Delta t$ (s)	$^{240}\text{Pu-eff}$ (g)	Singles (s <sup>-1</sup> )	Doubles (s <sup>-1</sup> )	Triples (s <sup>-1</sup> )	$\alpha$	Isotopics <sup>a</sup> $\alpha$	$M$	Doubles $^{240}\text{Pu-eff}$
A1-078	100 x 50	0.0888	99.39	9.97	2.30	1.037	0.981	1.00	112.3
5 MOX pellets	30 x 50	0.2431	265.80	27.96	6.40	0.939	0.941	1.00	115.0
STD Ash-1	46 x 100	1.2217	2 199.2	131.9	28.92	2.378	1.19	1.005	108.0
STD SGA-100	140 x 50	3.61	10 031.	414.5	97.5	3.962	2.55	1.009	114.8
*Alpha calculated for pure oxide matrix.									

additional carbon, calcium, oxygen, etc., increase the  $(\alpha, n)$  reaction rate compared with a pure  $\text{PuO}_2$  sample, and the multiplicity analysis calculates  $\alpha$  based on the higher moments in the neutron distribution.

If there is no multiplication in the samples, the ratio of  $T/(1 + \alpha)$  is a linear function of the  $^{240}\text{Pu-eff.}$  mass. Figure 18 shows a plot of the data in Table V and we see the almost-linear relationship between  $T/(1 + \alpha)$  and  $^{240}\text{Pu-eff.}$ , but with a small amount of multiplication-induced increase in  $T$  for the 100-g sample. The ash and diatomaceous earth matrix fillers dilute the high-mass samples by more than an order of magnitude. The good fit in Fig. 18 verifies that the large  $\alpha$  values calculated by the multiplicity analysis are accurate for these samples.

**SUMMARY**

The PSMC was designed to be highly efficient to give good counting statistical precision on the triples counts in reasonable time intervals. A typical high-burnup MOX sample containing a few hundred grams of plutonium gives 1% to 2% precision in a 1000-s measurement.

The PSMC can be used for small samples and pure samples using the conventional two-parameter assay. For impure samples, the multiplicity analysis can be used to reduce the

SUMMARY  
(cont.)

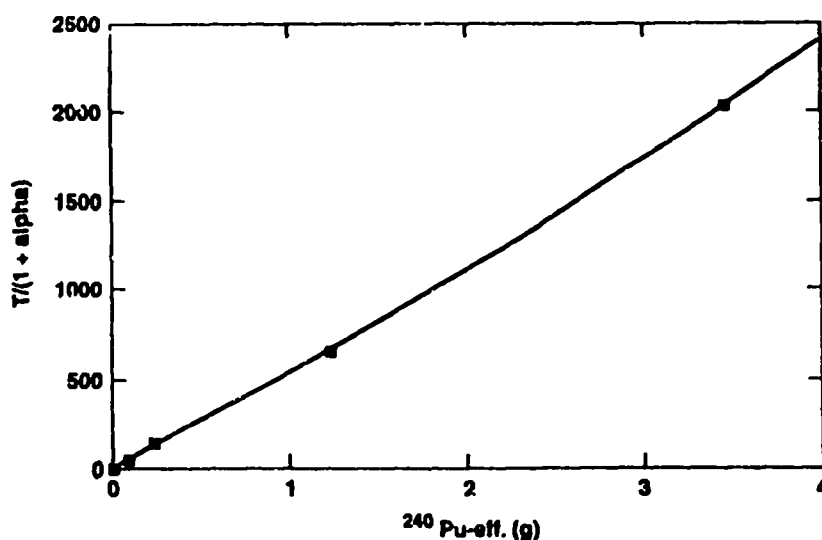


Fig. 18. The totals rate corrected for the  $\alpha$  value  $[T/(1 + \alpha)]$  vs the  $^{240}\text{Pu}$ -eff. mass for impure plutonium mixtures.

errors from incorrect  $\alpha$  values calculated from the isotopic ratios. For large MOX samples ( $\geq 3$  kg of plutonium), the errors from the multiplicity analysis become excessive, and the conventional coincidence analysis usually gives more accurate results.

The PSMC will be evaluated by the IAEA under field conditions beginning in September 1992.

## ACKNOWLEDGMENTS

The authors thank R. A. Augustson, G. W. Eccleston, and N. Ensslin for their support and useful advice during the course of the PSMC project. The acceptance testing and calibration of the PSMC was done by R. Abedin-Zadeh, P. Ammann, Y. Kulikov, H. Schreiber, and V. Siregar of the IAEA.

Support for the multiplicity counter's basic design and software was provided by the U.S. Department of Energy, Office of Safeguards and Security. Funding for the PSMC fabrication, testing, and installation was provided by the Program of Technical Support (POTAS) to the IAEA.

## REFERENCES

1. M. S. Krick and J. E. Swansen, "Neutron Multiplicity and Multiplication Measurements," *Nucl. Instrum. Methods* **219**, 384-393 (1984).
2. D. G. Langner, M. S. Krick, and N. Ensslin, "Pyrochemical Multiplicity Counter Design," *Proc. 31st Annual Meeting of the Institute of Nuclear Materials Management (INMM)*, Northbrook, Illinois, 1990), Vol. 19, pp. 411-415.
3. J. F. Briesmeister, Ed., "MCNP - A General Purpose Monte Carlo Code for Neutron and Photon Transport," Los Alamos National Laboratory report LA-7396-M, Version 3B (July 1988).
4. H. O. Menlove, R. Palmer, G. W. Eccleston, N. Ensslin, "Flat-Squared Counter Design and Operation Manual," Los Alamos National Laboratory report LA-11635-MS (July 1989).
5. J. E. Swansen, "Deadtime Reduction in Thermal Neutron Coincidence Counter," Los Alamos National Laboratory report LA-9936-MS (March 1984).
6. H. O. Menlove and J. E. Swansen, "A High-Performance Neutron Time-Correlation Counter," *Nucl. Technol.* **71**, 497-505 (November 1985).
7. N. Dytlewski, "Dead-time Corrections for Multiplicity Counters," *Nucl. Instrum. Methods* **A305**, 492-494 (1991).